Molar volume minimum and adaptative rigid networks in relationship with the intermediate phase in glasses

C. Bourgel,[1,2] M. Micoulaut,[3] M. Malki,[1,2] and P. Simon[1,2]
[1]*CNRS, UPR 3079 CEMHTI, 1D Avenue de la Recherche Scientifique, 45071 Orléans Cedex 02, France*
[2]*Université d'Orléans (Polytech'Orléans, Faculté des Sciences), BP 6749, 45072 Orléans Cedex 02, France*
[3]*Laboratoire de Physique Théorique de la Matière Condensée, UPMC-Paris 6, CNRS UMR 7600, Boite Postale 121 4, Place Jussieu, 75252 Paris Cedex 05, France*

(Received 17 June 2008; revised manuscript received 8 September 2008; published 21 January 2009)

We propose that the molar volume minimum observed in barium silicate glasses $(1-x)SiO_2-xBaO$ is related to the onset of an adaptative rigid glassy network. We obtain in the compositional window $29\%<x<33\%$ a dramatic decrease in stressed rigid local units from the Raman analysis and at $x=31\%$ the onset of barium ionic conduction. A random bond model [J. Barré *et al.*, Phys. Rev. Lett. **94**, 208701 (2005)] and constraint counting algorithms permit defining of the free energy of the system, and analyzing of the elastic nature of three compositional ranges of interest: a stressed rigid phase at low x, a flexible phase at high x, and a stress-free intermediate phase where space filling is optimized.

DOI: 10.1103/PhysRevB.79.024201 PACS number(s): 61.43.Fs, 63.50.−x

I. INTRODUCTION

The molar volume of binary-alloy liquids and glasses does not always display a monotonic behavior with alloy composition. For instance, molar volume minima have been reported for a certain number of glassy systems that underscore the tendency of a network to densify its structure in selected compositional ranges.[1] While this is a rather well documented and debated issue in alkali germanates,[2] little is known about the same tendency in silicate glasses and liquids[3] although the precise knowledge and the origin of compositional trends in molar volume have some obvious implications in geochemistry and Earth Sciences in general.

In the literature, a principle for compactness optimum has been invoked from an elegant argument stating that a mechanical stability[4] is reached when the number density of mechanical constraints n_c arising from interatomic bond-bending and bond-stretching forces equals the number of degrees of freedom. This mechanical stability criterion has been later identified with a rigidity transition[5] at which the number density of (low-frequency) floppy modes $f=3-n_c$ vanishes. It implies that the volume contraction is linked with tight bonding and shorter bond lengths when the number density of constraints matches exactly the number of degrees of freedom. However, space-filling tendency is obviously the consequence of a collective behavior and cannot be simply handled from global (or mean-field) approaches.[4,5] In chalcogenide network glasses, it has been observed that space-filling compositional windows[6,7] were correlated with thermally reversing windows [or rigid intermediate phases (IP)] obtained from complex heat-flow measurements at the glass transition.[8] These windows are located around the network mean coordination number $\bar{r}=2.4$, and are found between the flexible (where $n_c<3$) and the stressed rigid phase ($n_c>3$) of glasses.[9–13]

Do such correlations exist in other types of networks such as the oxides or ionic conductors? Recent molecular-dynamics simulations of densified silicas have shown[14,15] that the balance between two structural mechanisms accommodating low (flexible) and high (stressed rigid) pressure applications could lead to a space-filling window, clearly related with a pressure-induced rigidity transition. Here it is shown that the correlation between space-filling windows and the intermediate phase also exist in rigidity induced by composition for an archetypal silicate system, the barium based glass. Our results therefore underscore the commonality of the physics driving the formation of intermediate phases in covalent-chalcogenide and ionic-oxide glasses, and the way (composition and pressure) space-filling windows can be achieved.

We describe experimental and theoretical results on barium silicates of the form $(1-x)SiO_2-xBaO$ from Raman spectroscopy, ionic conduction, and a random bond model,[11] which show that the observed molar volume minimum is located in the intermediate phase which results from the network adaptation leading to a rigid and almost stress-free network within the compositional window $29\%<x<33\%$. In this respect, barium silicates display very common features with chalcogenide network glasses. Beyond this main issue, the present paper shows also how the intermediate phase in glasses can be detected when its most obvious signature from heat-flow measurements cannot be provided. Barium silicates and geological glasses in general have glass transition temperatures that exceed by far the highest accessible temperature of the calorimetric setup[8] used for the heat-flow measurements. One has therefore to find alternative experimental signatures for the intermediate phase in these peculiar high-temperature glassy systems. Barium silicate glasses and melts have received little attention compared to alkali silicates although the role of alkaline-earth silicates tends to be even more important as network modifiers in natural systems than alkali metals. Any new insight into the structure, the thermal behavior, and/or the electrical transport behavior is therefore welcome.

The present paper is organized as follows: in Sec. II, we show the molar volume results, and describe the experimental data obtained in Raman scattering and conductivity measurements together with the estimate of the total number den-

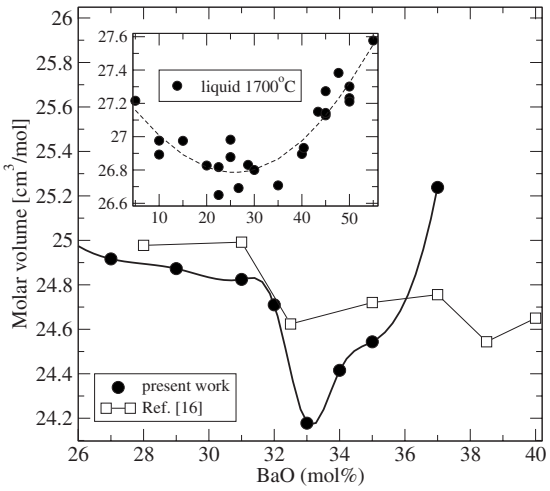

FIG. 1. Molar volume of barium silicate glasses $(1-x)SiO_2-xBaO$ as a function of barium composition. Additional data are from Bansal and Doremus (Ref. 16). Error bars are of the size of the symbols. The inset shows the molar volume (Ref. 17) of the liquid at 1700 °C.

sity of mechanical constraints from Maxwell counting. Section III is devoted to the application of an adaptative random model[11] to the present barium silicates. Results of the model are put in contrast with the experimental findings. We discuss the latter in Sec. IV and collected molar volume data for various oxide and chalcogenide glasses are shown. They highlight the fact that the present enunciated relationship between molar volume minimum and the intermediate phase is not restricted to the present investigated system. We finally summarize our results and sketch some more general conclusions.

II. EXPERIMENTAL

A. Results

A set of glasses has been prepared by mixing SiO_2 (99.99%) and $BaCO_3$ (99.99%) powders in the stoichiometric proportions. For each composition, the mixture was melted in a platinum crucible at 1650 °C for 2 h, and quenched by pressing the melt between two copper plates. The glass transition temperatures were found at about 720 °C.

The complex electrical conductivity was measured on Pt-metallized disks (1 mm in thickness and 12 mm in diameter) using a Solartron SI 1260 impedance meter in the frequency range of 1 Hz–1 MHz from room temperature up to T_g+60 °C. Raman spectra were obtained on a Jobin-Yvon T64000 spectrometer with charge-coupled device (CCD) detection and BX40 Olympus microscope. The excitation wavelength was the 514.532 nm argon line of a Coherent Innova 70 Spectrum laser.

The starting point of the present study is the behavior of the molar volume (measured by buoyancy method) with composition displayed in Fig. 1. Our results show a minimum at 33% barium content with a molar volume of 24.1 cm^3/mol at this composition. Precursive behavior is

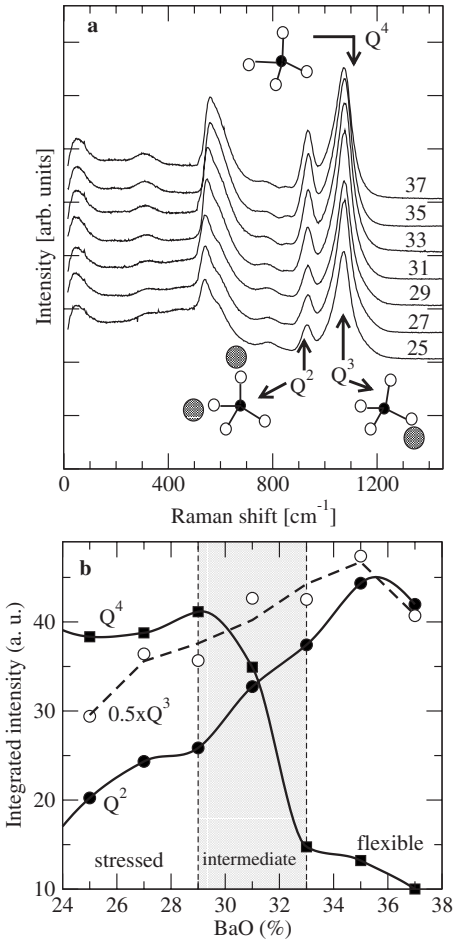

FIG. 2. Panel a: Raman line shapes of $(1-x)SiO_2-xBaO$ glasses with the definition of the relevant modes and corresponding structural units (barium atoms are in gray) used in the discussion (see text for details). Panel b: Integrated intensity from Raman deconvolution showing the behavior of the Q^n speciation with barium composition. The dashed region between 29% and 33% corresponds to the intermediate phase.

already found in the liquid[17] at 1700 °C (inset of Fig. 1). The Raman spectra for various compositions [Fig. 2(a)] have been deconvoluted to obtain Fig. 2(b). Details of the method and measurements (Bose-Einstein correction, peak deconvolution, logarithmic-normal law for low frequencies, etc.) can be found elsewhere.[18,19] We specifically focus on the bands at 1110, 1070, and 920 cm^{-1} that are, respectively, identified (see also Ref. 20) with the population of Q^4, Q^3, and Q^2 units corresponding, respectively, to the $SiO_{4/2}$ (the basic tetrahedron of silica), $BaSiO_{5/2}$, and Ba_2SiO_3 units. The superscript in Q^n stand here for the number n of bridging oxygens (BOs) connecting the network whereas oxygen connected to barium atoms [one on a Q^3, two on a Q^2, see also Fig. 2(a)] are usually termed as nonbridging oxygens (NBOs). The integrated intensity of these Raman bands (proportional to their probability of occurrence) is represented in Fig. 2(b) as a function of barium content. It shows that the population of Q^4 species decreases dramatically between the barium compositions of 29% and 33%, whereas the Q^2 unit increases substantially inside the same compositional interval, and up

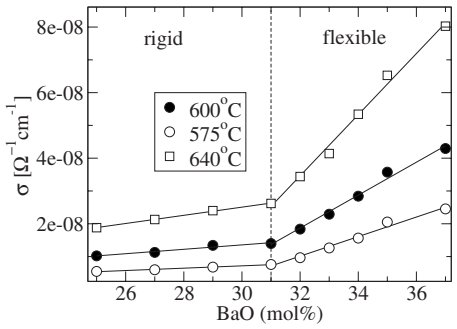

FIG. 3. Dc conductivity of barium silicates $(1-x)SiO_2-xBaO$ as a function of the barium composition x. Straight lines are guides for the eyes. The vertical broken line marks the approximate onset of conduction.

to 35% before starting to decrease as Q^1 units start to appear. Finally, Fig. 3 shows the dc conductivity of vitreous barium for different temperatures. Around the composition of 31%, one observes a sudden increase in the conductivity which is multiplied by a factor of four with only 5% addition more of BaO.

From the three figures, we can define three barium compositional intervals: a first one for $x<29\%-31\%$ where the network is made of a majority of Q^4 and Q^3 units, and where the ionic conductivity is weak. An intermediate region $29\%-31\%<x<33\%$ where the local structure is changed in a rather deep fashion and where the molar volume decreases to its minimum. Finally, a third compositional interval is found for $x>33\%$ where the abrupt decrease in Q^4 units found between 29% and 33% barium is reduced. This suggests that the underlying nature of the network has been substantially modified. We identify these compositional intervals, respectively, with the stressed rigid, the intermediate, and the flexible phases of glasses.

The location of the IP deserves some additional comments. In thermal measurements such as those reported in Ref. 8, it is rather hard to determine accurately the wall location of the intermediate phase unless one has many compositions over narrow composition ranges. This remains also true for conductivity measurements and distinct changes in regime over the three elastic phases, which seems at present only allowed for highly silver conductive glasses.[21] Our conductivity results (Fig. 3) are three orders of magnitude lower than those reported in Ref. 21, and therefore only parallels the behavior of silver electrolytes in the stressed and the flexible phases, i.e., an almost constant value for σ in the stressed rigid phase, and a rapid increase in the flexible phase.

In many systems,[22,23] it is difficult to measure the boundaries of the IP from Raman scattering. This is mostly the case when modes are not clearly resolved, making mode frequency measurements less reliable. Fortunately, the behavior with composition of our resolved frequency modes clearly shows two changes in behavior, and defines the boundaries of an intermediate phase between 29% and 33%. In this respect, the behavior is very close to that observed in Si-Se and Ge-Se network glasses[24,25] where the IP is better fixed from Raman elastic thresholds than from the reversibility windows

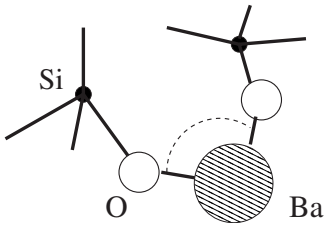

FIG. 4. Part of the barium silicate network showing the silicon-NBO sequence around a barium atom. With broken barium bending constraints, the NBOs connecting two rigid tetrahedra has also broken bending constraints.

(i.e., from calorimetry). These thresholds correspond, as best as one can tell, to the walls of the reversibility windows.

In summary, from Fig. 1, one can conclude that an IP is found between 31% and 33%, and from Fig. 2 between 29% and 33%. In contrast with the data on silver phosphate conduction,[21] a single threshold composition is found for the barium conductivity at 31%.

B. Global Maxwell counting

A preliminary piece of evidence for our proposal is given by global Maxwell (bond-stretching, α, and bond-bending, β) constraint counting that leads to the estimation of the mean-field location of the rigidity transition.[5] We consider the $BaO-SiO_2$ system as a network of N atoms with three kinds of atoms with a given coordination number and concentration given by stoichiometry. One has first to remark that, although the structure is modified in a rather deep fashion by network depolymerization, the $SiO_{4/2}$ tetrahedral environment is preserved in these glasses because of the sp^3 hybridization of silicon. This defines rather accurately the silicon and oxygen bondings, and leads to sharp O-Si-O and Si-O-Si angular distributions, respectively, peaked[26] at 109° and 144°. Modifier ions do not follow such strong chemical bonding conditions and they distribute therefore over much broader angular ranges.[27] This means that corresponding bond-bending restoring forces are stronger for silicon and oxygen than for barium. A more detailed examination of the bond angle distributions shows that barium centered and barium-oxygen connected bond angles display wide excursions[28] around their mean value as manifested by, e.g., the full width at half maximum σ_{i-j-k} of the angular distribution ($\sigma_{\text{O-Ba-O}}=90°$ against $\sigma_{\text{Si-O-Si}}=25°$). This implies that barium mechanical constraints should be restricted simply to bond stretching with their bond-bending constraints being broken.

Furthermore, the NBOs connected to bariums should have broken bond-bending constraints as well. Indeed, a sequence of atoms Si-O-Ba-O-Si forms a chain (Fig. 4) with O-Si-O angles being maintained (sp^3 hybridization), and it seems rather unlikely that the bond angle Si-O-Ba is fixed by a constraint with the allowed bending motion of the barium atoms. This can also be detected from the Si-Ba-Si (and similarly with the Ba-Si-Ba) bond angle distributions[28] which display rather large full widths at half maximum, very similar to the one of O-Ba-O. With this in mind, and taking

the coordination numbers of silicon, barium,[29] and oxygen as, respectively, four, two, and two, one can evaluate the fraction of floppy modes per atom. From the chemical formula $(1-x)SiO_2-xBaO$, one can compute the number of atoms of the network which is $N=(3-x)\mathcal{N}$/mol of chemical formula, and the number of α and β constraints[30] is $N_c=(11x-10)\mathcal{N}$. Here $\mathcal{N}$ stands for Avogadro's number. This leads to

$$f = F/N = \frac{1}{N}(3N - N_c) = 3 - n_c = \frac{7x-2}{3-x}, \tag{1}$$

which vanish at $x=x_c=2/7$, i.e., at 28.5% barium. Maxwell constraint counting therefore predicts a rigid to flexible transition at a barium concentration of 28.5%. Glass forming tendency is optimized[4] at this composition in harmony with current experimental observation.[33]

III. ADAPTATIVE SILICATE NETWORKS

Using the preliminary result of Eq. (1), our first piece of evidence for the intermediate phase comes from a random bond model that builds on the counting scheme above, and the approach introduced for III-I networks.[11] From the statistics $\{x_n\}$ of the Q^n $(n=2,3,4)$ with coordination number $r=n$ displayed in Fig. 2(b), we consider all possible bonding types, i.e., between the two 4 species (4–4), one 4 and one 3 (4–3), etc. In the randomly bonded case, it is rather simple to obtain the probabilities for the Q^i-Q^j bonds,

$$p_{ij} = \frac{(2-\delta_{ij})ijx_ix_j}{\left(\sum_{i=2}^{4} ix_i\right)^2} = p_{ij}^*, \tag{2}$$

leading, for instance, to

$$p_{43} = \frac{24x_4x_3}{(4x_4+3x_3+2x_2)^2} = p_{43}^*, \tag{3}$$

$$p_{42} = \frac{16x_4x_2}{(4x_4+3x_3+2x_2)^2} = p_{42}^* \tag{4}$$

for, respectively, a Q^4-Q^3 and a Q^4-Q^2 bonding type. Here, the symbol * in the right-hand side of Eq. (2) denotes the fact that it is a random distribution without any energetical influence, the probabilities being just given by combinatorial factors arising from the local connectivity of the species.

Since we have identified (from, e.g., Fig. 3) that the silica-rich and barium-rich glasses were, respectively, stressed rigid and flexible, the network stress should increase when the barium concentration is decreased. We can write this more precisely by defining a stress energy $U(x)$ (stress costs energy) for a given network configuration that will be proportional to the number density of redundant constraints in the system, i.e., $-f$, which are constraints that cannot be fulfilled. Moreover since in the flexible phase, there are no redundant constraints, the stress energy should be zero at high barium concentration when all constraints can be fulfilled. Note that a perfectly symmetric approach can be used by defining a floppy mode energy instead of a stress energy.[34] In this case, it is proportional to f and vanishes when the network becomes rigid. A more precise description of the stress energy that would go beyond the general framework introduced in Ref. 11 is rather difficult. In fact, measurements on the elastic properties (bulk modulus, shear modulus, and sound velocities) of barium silicates[35] have been only performed for one composition (33% barium) and cannot be used to estimate the stress energy as a function of barium content (or cross-link density).

In general, one needs to establish a hierarchical approach for the computation of the stress energy as it is well known that bond-bending energies are weaker when compared to bond-stretching energies.[36] This separates stress energy into two main contributions: stretching and bending with other contributions arising from more weaker forces being ignored.[37] Based on the Maxwell counting scheme, in the present barium system, the corresponding contributions n_c^α and n_c^β to the stress energy are

$$U(x) = n_c^\alpha(x) + n_c^\beta(x) - 3 = \frac{4-2x}{3-x} + \beta\frac{7-8x}{3-x} - 3, \tag{5}$$

with β supposed to be less than one, i.e., signifying that bending forces should be weaker than stretching forces. We have checked that, in order to have a vanishing of f [or $U(x)$] in the barium compositional region of interest (i.e., approximately between [0.1, 0.4]), one needs to have a weight between stretching and bending contributions of approximately 1:0.8, i.e., $\beta \simeq 0.8$. This is not very surprising. Indeed, as the weak angular constraints involving barium or NBOs are broken, the major contribution to n_c^β comes from the silicon angular constraints, which have a rather high energy, as tetrahedral ordering (sp^3 hybridization) needs to be maintained. Thus it is reasonable to treat the remaining bending (Si and BO) and the stretching energies as about the same in the barium system. One has therefore to keep in mind that, if a distinction is made between stretching and bending energies (i.e., taking $\beta<1$), the location of the rigidity transition given by Eq. (1) will be shifted to lower concentrations, the same as the results given below.

For a given configuration of the network, an entropy can be defined. This finally leads to the definition of the free energy $F_{(l)}$ of the system that takes into account both the configurational entropy of the network and the stress energy. This free energy can be computed for different types of approximations l. In fact, the crudest approximation ($l=0$, i.e., concentration based) involves only the macroscopic concentration x. In this case, the stress energy follows the counting that leads to f from Eq. (1), and the ideal-gas entropy:

$$F_{(0)}(x) = -f + k_BT[x\ln x + (1-x)\ln(1-x)], \tag{6}$$

where T represents the fictive temperature, i.e., the temperature of formation of the network.[38] This temperature is usually slightly higher than the glass transition temperature (here $T_g \simeq 720$ °C for all compositions, i.e., 85 meV). In the present construction, however, k_BT is dimensionless, such as f or $F_{(0)}$. The vibrational free energy coming from the harmonic-oscillator contributions of the Q^i species with their

corresponding mode frequencies ω_i=1110, 1070, and 920 cm^{-1} depends rather weakly on the barium composition because T and ω_i are nearly constant. In the forthcoming, we therefore do not consider this particular contribution and focus only on an energy arising from extra constraints and on the configurational entropy.

The next approximation (l=1, i.e., specie based) involves the distribution of local structures [Q^n (n=2,3,4), Fig. 2(b)]. The number of redundant constraints leading to a stress energy can be computed from the statistics $\{x_n\}$ and the entropy follows a Bragg-Williams-type expression,

$$U_{(1)}(x) = \frac{\sum_{i=2,3,4} n_{c(i)} x_i}{\sum_{i=2,3,4} n_i x_i} - 3, \tag{7}$$

$$F_{(1)}(x) = \frac{\sum_{i=2,3,4} n_{c(i)} x_i}{\sum_{i=2,3,4} n_i x_i} - 3 + k_B T \sum_{i=2,3,4} x_i \ln x_i, \tag{8}$$

where $n_{c(i)}$ are the number of constraints computed on the species Q^i and n_i their number of atoms (e.g., $n_{c(4)}/n_4$ =3.67 for the stressed rigid Q^4). Finally, we can use the distribution $\{p_{ij}\}$ whose expressions in the random case are given by Eq. (2). It is a bond based (l=2) approximation, and one has, similarly to Eq. (8)

$$F_{(2)}(x) = \frac{\sum_{i,j=2,3,4} (n_{c(i)} + n_{c(j)}) p_{ij}^*}{\sum_{i=2,3,4} (n_i + n_j) p_{ij}^*} - 3 + k_B T \sum_{i,j=2,3,4} p_{ij}^* \ln p_{ij}^*. \tag{9}$$

Results for the free energy are displayed in Fig. 5. They show for $F_{(0)}$ and $F_{(1)}$ a minimum in the region 30%–35% of barium, close to the threshold observed experimentally. For the random bond case (solid line of $F_{(2)}$ in Fig. 4), deviation from randomness needs to be achieved in order to shift the free-energy minimum to higher concentrations. Obviously, the random bond case underestimates the stress present in the network as the vanishing of the stress energy occurs at lower x. The probability of stress needs to be rescaled.

The level of organization of the network can therefore be tuned by introducing a parameter $\alpha=(p_{44}+p_{43})/(p_{44}^*+p_{43}^*)$ that changes the probability of finding stressed rigid bonding types (4–4 and 4–3), and α denotes in this case a measure of the network adaptation (Fig. 5, broken lines) as it rescales the random probability of having stress. In fact, an enumeration of mechanical constraints shows that, among all possible bonding types Q^i-Q^j, only two are stressed rigid: the Q^4-Q^4 (n_c=3.67 per atom, see Table I) and the Q^4-Q^3 bonding types (n_c=3.21 per atom). Figure 5 shows in fact that the location of the rigidity transition is closer to the observed threshold at 29% barium when α is smaller than one. The inset of the figure furthermore shows that the increase in α leads to a shift of the rigidity transition composition x_R to higher x. Finally, we note that, for $\alpha \neq 1$, the region where f is close to zero and where the configurational entropy is maximum coincides with a maximum in stress-free (isostatically rigid) bonding types (Fig. 5, right axis). At around 35% barium, around 75% of the network is isostatically rigid and the free energy of the system remains constant. Note also that, for higher barium concentrations ($x>45\%$), one cannot neglect Q^1 units (a $Ba_3Si_2O_3$ unit) anymore so that the minimum seen in $F_{(2)}(x)$ at around 47% barium highlights the limitation of the approach.

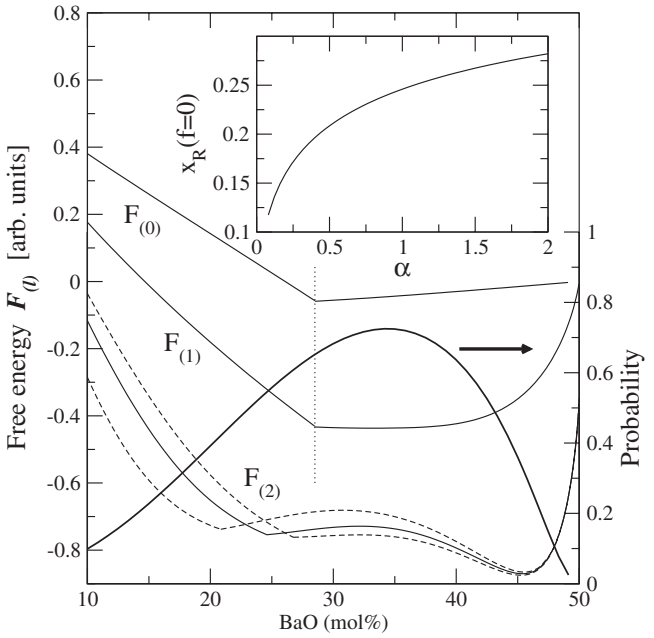

FIG. 5. Free energies $F_{(l)}$ of the system (solid curves) as a function of barium concentration for various approximations: concentration based (l=0), species based (l=1) and random bond based (l=2, solid line). The broken curves correspond to adaptative random bond networks (α=0.5 and α=1.5) at l=2. The vertical dotted line shows the location of the Maxwell rigidity transition at x_c=28.5%. Here k_BT=0.5. The inset shows the location of the rigidity transition as a function of the adaptation of the network (α, see text for details). Right axis: probability of finding isostatically rigid bonding types for α=0.5.

IV. DISCUSSION

A. Evidence for stress from experiments

Concerning the order of the underlying phase transitions that bound the intermediate phase, it has been stressed that

TABLE I. Number of constraints of all possible Q^i-Q^j pairs. Note that only the 4–4 and 4–3 pairs are stressed rigid.

Q^i-Q^j pair	Constraints/atom	Elastic nature
4–4	3.67	Stressed
4–3	3.21	Stressed
4–2	2.88	Flexible
3–3	2.88	Flexible
3–2	2.61	Flexible
2–2	2.40	Flexible

the higher-coordinated side should be a first-order stress transition while the lower coordinated side is a second-order rigidity transition.[25] Chalcogenide network glasses show indeed a jump in some characteristic Raman mode frequencies ν at the stress transition,[39] in agreement with theory.[13] Furthermore, the corresponding optical elasticities ν^2 display a power-law variation[5] in $(\bar{r}-\bar{r}_c)$ or $(x-x_c)$ with an exponent close to 1.5. Here, we obtain from theory for the higher-coordinated side (i.e., low barium content) a second-order stress transition only, corresponding to the vanishing of the stress energy. This contrasts with the previous findings in the chalcogenides. However, our Raman results (Fig. 2) show clearly that there is no jump in typical mode frequencies, linewidth, or integrated intensity at the observed thresholds of 29% and 33%. The typical lines shown in Fig. 2(a) have frequencies (or linewidths) that show neither threshold behavior at the composition of interest nor a jump at the 29% barium stress transition.

Evidence for an intermediate phase in the compositional region $0.29<x<0.33$ is also provided by the Q^n statistics displayed in Fig. 2. Enumeration of Lagrangian constraints on the different types shows that the Q^4 species are stressed rigid ($n_c=3.67$) whereas Q^2 and Q^3 are flexible (respectively, $n_c=2.40$ and $n_c=2.88$). For the latter, one should note that it is still rather close to the optimal constrained structure of $n_c=3$. The dramatic decrease in the Q^4 starting from $x\simeq 29\%$ implies the breakdown of stressed rigidity. On the other hand, with a large fraction of Q^3 species present in the network in the compositional range of 29%–32%, one sees that the network can be considered close to the intermediate state ($n_c\simeq 3$). From the behavior of the stressed rigid unit Q^4, one can clearly conclude that stress is decreasing in the IP, in harmony with previous findings.[9,39]

Our last piece of evidence is provided by the conductivity measurements of Fig. 3 that parallels to some extent results on silver phosphate systems.[21] Distinct regimes in ionic conduction can indeed be found depending on the nature of the network backbone (flexible, intermediate, stressed rigid), and the location of the boundaries map onto the boundaries of the thermally reversing window. In the flexible phase, conductivity onsets due to occurrence of floppy modes that facilitate the motion of the cations within the structure. Figure 3 shows this kind of onset at a composition slightly higher than the one that would be expected from the Raman analysis.

B. Space-filling and intermediate phases

Can these conclusions be put in connection with the observed molar volume minimum? In oxide systems such as SiO_2 based glasses, space-filling tendencies can be hardly inferred from a purely structural basis. In fact, because of the restricted range of permissible intertetrahedral Si-O-Si angles that lead also to a limited tolerance in the O-O bond distance, it appears to be rather difficult to build model random networks that are able to fill optimally space. In molecular simulations, this can be only achieved from a local distortion of the $SiO_{4/2}$ tetrahedron under pressure.[14] However, the transformation of BO to NBO with increasing modifier composition usually gives rise to contraction as manifested[40,41]

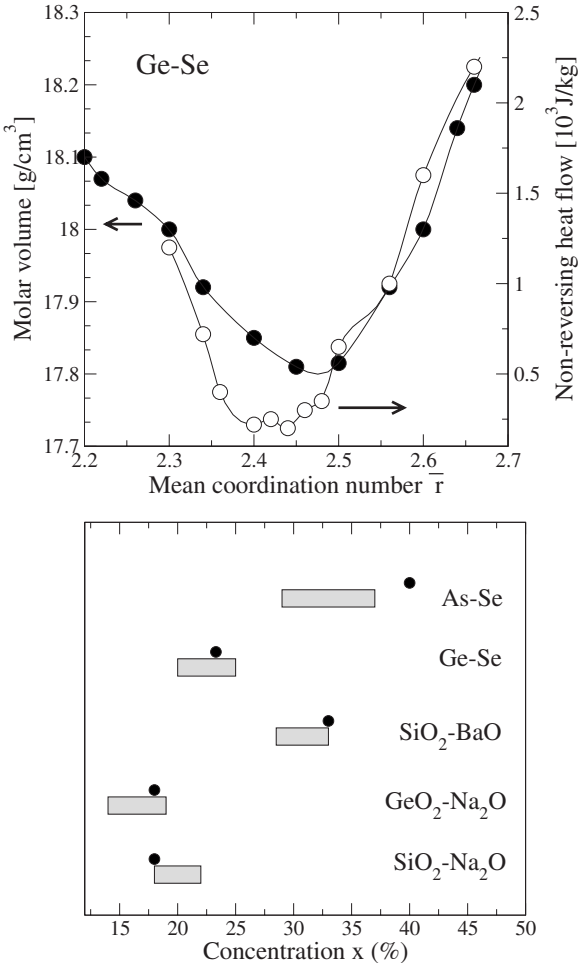

FIG. 6. Top: Molar volume and nonreversing heat flow (Refs. 42 and 43) (right axis) as a function of germanium concentration x in a binary Ge-Se glass. Bottom: Location and width of the intermediate phase for modified glassy and liquid chalcogenide and oxide systems compared with the location (circles) of a molar volume minimum. Data are from Refs. 23, 31, and 42–47. Here x represents the concentration of modifier atom (or molecule): Na_2O, BaO, Ge, and As.

by the reduction in length between a metal-BO distance and a metal NBO. But as the fraction of metal-NBO bonds steadily increases at the expense of metal-BO bonds, there is no obvious reason why the glass should display a contraction maximum.

In Fig. 6 (top), we have represented as a function of the network mean coordination number $\bar{r}$, the molar volume V and the nonreversing heat flow ΔH_{nr} of a Ge-Se system. Clearly, the trends are similar and the composition at which V and Δ_{nr} are minimum is close. Also since the interval where ΔH_{nr} is minimum corresponds to the intermediate phase (whose boundaries are also determined from vibrational thresholds, as discussed previously), one can conclude that an argument based on partial molar volume combined with the contraction of bond lengths cannot account for the observed minimum in V. Moreover, there is no observed bond distance contraction in Ge-Se with composition.[48]

In silicates, it has been also often stressed that since the partial molar volume of SiO_2 was decreasing with network

depolymerization (or modifier content), one would expect the molar volume to decrease with the fraction of Q^4 units.[3] Moreover as usual modifiers have a partial molar volume larger than the molar volume of SiO_2, there must be a special point in composition where a molar volume minimum is reached. This argument runs against the observed behavior in network chalcogenides which display a molar volume decrease (Fig. 6, top) although the network is polymerized by, e.g., germanium or arsenic atoms, i.e., it is increasing its connectivity.

Another reason put forward[49] deals with the free volume of a glass defined by $V_f = \Delta\alpha T_g$, where $\Delta\alpha$ is the difference in thermal-expansion coefficient between the supercooled liquid and the glass. In fact, for a glass having a large free volume in the base network, there can be a possibility that the system will display space filling for selected compositions at which local stresses induced by differences in atomic sizes are able to allow compaction. One would therefore expect that base glasses with a large free volume will compact more easily. Observation of Fig. 6 (bottom) shows that this argument cannot account for glasses displaying very different free volumes for the basic network former. Silica and germania have a respective free volume V_f of about 0.001 (Ref. 50) and 0.04 (Ref. 49) much smaller than chalcogenides 0.1 (Ref. 51) although all can lead to space filling with addition of a modifier atom or molecule. However, one can notice from Fig. 6 that compositional windows where the nonreversing heat flow vanishes (the intermediate phase) correlate with the composition for which a molar volume minimum is found. In chalcogenides, the minimum is found on the higher-coordinated (stressed) side of the IP whereas in oxide glasses, its location lies rather on the flexible side.

V. SUMMARY AND CONCLUSIONS

We have shown that a molar volume minimum can be found in barium silicate glasses, a very important system in Earth Sciences. A random bond model shows that a stress on the flexible transition occurs in the vicinity of the molar volume minimum composition. Raman spectroscopy shows evidence for the rapid loss of stressed rigidity in the interval $29\% < x < 33\%$, whereas onset of conduction is found at 31%. Adaptative networks are necessary at the one bond approximation level to recover the location of the rigidity transition and the IP. Free energy minimum and rigidity transition coincide in the intermediate phase were the network is mostly isostatically rigid. The rapid increase in the conductivity at larger barium compositions is a signature that the network flexibility is now promoting conduction.

Finally, it opens also a perspective that goes beyond network glassy materials. Indeed, since rigidity can be also found in soft solids and[52] in relationship with close packing of (soft or hard) spheres, characterizing the connection between the absence of stress and the space-filling properties in glasses should help for a better understanding of other noncovalent glassy materials such as colloids.

ACKNOWLEDGMENTS

It is a pleasure to acknowledge ongoing discussions with P. Boolchand, B. Goodman, D. R. Neuville, and P. Richet. This work has been supported by a CNRS grant France/Etats-Unis.

[1] P. L. Higby and I. D. Aggarwal, J. Non-Cryst. Solids **163**, 303 (1993).
[2] G. S. Henderson and M. E. Fleet, J. Non-Cryst. Solids **134**, 259 (1991).
[3] P. Richet and B. O. Mysen, *Silicate Glasses and Melts: Properties and Structure* (Elsevier, Amsterdam, 2005).
[4] J. C. Phillips, J. Non-Cryst. Solids **34**, 153 (1979).
[5] M. F. Thorpe, J. Non-Cryst. Solids **57**, 355 (1983).
[6] A. N. Sreeram, A. K. Varshneya, and D. R. Swiler, J. Non-Cryst. Solids **128**, 294 (1991).
[7] J. C. Phillips, arXiv:cond-mat/0606418 (unpublished).
[8] S. Chakravarty, D. G. Georgiev, P. Boolchand, and M. Micoulaut, J. Phys.: Condens. Matter **17**, L1 (2005); P. Boolchand, D. G. Georgiev, B. Goodman, and J. Optoelectr, J. Optoelectron. Adv. Mater. **3**, 703 (2001).
[9] F. Wang, S. Mamedov, P. Boolchand, B. Goodman, and M. Chandrasekhar, Phys. Rev. B **71**, 174201 (2005).
[10] M. F. Thorpe, D. J. Jacobs, M. V. Chubynsky, and J. C. Phillips, J. Non-Cryst. Solids **266-269**, 859 (2000).
[11] J. Barré, A. R. Bishop, T. Lookman, and A. Saxena, Phys. Rev. Lett. **94**, 208701 (2005).
[12] M. V. Chubynsky, M. A. Brière, and N. Mousseau, Phys. Rev. E **74**, 016116 (2006).
[13] M. Micoulaut and J. C. Phillips, Phys. Rev. B **67**, 104204 (2003).
[14] K. Trachenko, M. T. Dove, K. D. Hammonds, M. J. Harris, and V. Heine, Phys. Rev. Lett. **81**, 3431 (1998).
[15] K. Trachenko, M. T. Dove, V. Brazhkin, and F. S. El'kin, Phys. Rev. Lett. **93**, 135502 (2004).
[16] N. B. Bansal and R. H. Doremus, *Handbook of Glass Properties* (Academic, New York, 1960).
[17] J. W. Tomlinson, M. S. R. Heines, and J. O. M. Bockris, Trans. Faraday Soc. **54**, 1822 (1958).
[18] M. Micoulaut, M. Malki, P. Simon, and A. Canizares, Philos. Mag. **85**, 3357 (2005).
[19] C. Bourgel, M. Malki, P. Simon (unpublished).
[20] J. D. Frantza and B. O. Mysen, Chem. Geol. **121**, 155 (1995).
[21] D. I. Novita, P. Boolchand, M. Malki, and M. Micoulaut, Phys. Rev. Lett. **98**, 195501 (2007).
[22] P. Boolchand, M. Jin, D. Novita, and S. Chakravarthy, J. Raman Spectrosc. **38**, 660 (2007).
[23] R. Rompicharla, D. I. Novita, P. Chen, P. Boolchand, M. Micoulaut, and W. Huff, J. Phys.: Condens. Matter **20**, 202101 (2008).
[24] D. Selvanathan, W. J. Bresser, and P. Boolchand, Phys. Rev. B **61**, 15061 (2000).
[25] P. Boolchand, X. Feng, and W. Bresser, J. Non-Cryst. Solids **293-295**, 348 (2001).
[26] R. L. Mozzi and B. E. Warren, J. Appl. Crystallogr. **2**, 164 (1969).
[27] G. N. Greaves and S. Sen, Adv. Phys. **56**, 1 (2007).

[28] H. Schlenz, A. Kirfel, K. Schulmeister, N. Wartner, W. Mader, W. Raberg, K. Wandelt, C. Oligschleger, S. Bender, R. Franke, J. Hormes, W. Hoffbauer, V. Lansmann, M. Jansen, N. Zotov, C. Marian, H. Putz, and J. Neuefeind, J. Non-Cryst. Solids **297**, 37 (2002).

[29] For a general discussion on coordination numbers, number of neighbors, and constraint counting, see M. Micoulaut, Am. Mineral. **93**, 1732 (2008).

[30] From $(1-x)SiO_2-xBaO$, one can split the chemical formula of the glass into BO and NBO contributions: $Si_{1-x}O^{BO}_{2-3x}$-$Ba_xO^{NBO}_{2x}$. Having, respectively, seven, two, one, and one constraints for silicon, BO, NBO, and barium atoms, we obtain the corresponding mechanical constraints $7-7x$, $4-6x$, $2x$, and x in the glass. Note that this constraint enumeration cannot be extrapolated down to $x=0$ because BO bending constraints are usually broken in SiO_2. For a detailed discussion, see M. Zhang and P. Boolchand, Science **266**, 1355 (1994). The present enumeration holds at least down to compositions such as $x=0.14$ as demonstrated from the observation of an IP in sodium and potassium silicates (Refs. 31 and 32).

[31] Y. Vaills, T. Qu, M. Micoulaut, F. Chaimbault, and P. Boolchand, J. Phys.: Condens. Matter **17**, 4889 (2005).

[32] M. Malki, M. Micoulaut, F. Chaimbault, and Y. Vaills, Phys. Rev. Lett. **96**, 145504 (2006).

[33] Z. U. Borisova, *Glassy Semiconductors* (Plenum, New York, 1981).

[34] G. G. Naumis, Phys. Rev. E **71**, 026114 (2005).

[35] N. Soga, H. Yamanaka, C. Hisamoto, and M. Kunugi, J. Non-Cryst. Solids **22**, 67 (1976).

[36] A. J. Rader, Brandon M. Hespenheide, Leslie A. Kuhn, and M. F. Thorpe, Proc. Natl. Acad. Sci. U.S.A. **99**, 3540 (2002).

[37] W. A. Kamitakahara, R. L. Cappelletti, P. Boolchand, B. Halfpap, F. Gompf, D. A. Neumann, and H. Mutka, Phys. Rev. B **44**, 94 (1991).

[38] F. L. Galeener, D. B. Kerwin, A. J. Miller, and J. C. Mikkelsen, Jr., Phys. Rev. B **47**, 7760 (1993).

[39] T. Qu, D. G. Georgiev, P. Boolchand, and M. Micoulaut, in *Supercooled Liquids, Glass Transition and Bulk Metallic Glasses*, MRS Symposium Proceedings No. 754, edited by T. Egami, A. L. Greer, A. Inoue, and S. Ranganathan (Materials Research Society, Pittsburgh, 2003), p. CC8.1.1.

[40] C. Huang and A. N. Cormack, J. Chem. Phys. **93**, 8180 (1990).

[41] C. Huang and A. N. Cormack, J. Chem. Phys. **95**, 3634 (1991).

[42] A. Feltz, H. Aust, and A. Blayer, J. Non-Cryst. Solids **55**, 179 (1983).

[43] X. Feng, W. J. Bresser, and P. Boolchand, Phys. Rev. Lett. **78**, 4422 (1997).

[44] A. L. Renninger and B. L. Averbach, Phys. Rev. B **8**, 1507 (1973).

[45] D. G. Georgiev, P. Boolchand, and M. Micoulaut, Phys. Rev. B **62**, R9228 (2000).

[46] Y. Bottinga and P. Richet, Geochim. Cosmochim. Acta **59**, 2725 (1995); R. Brückner, Glastech. Ber. **37**, 459 (1964).

[47] G. S. Henderson, J. Non-Cryst. Solids **353**, 1695 (2007).

[48] P. S. Salmon, J. Non-Cryst. Solids **353**, 2959 (2007).

[49] S. Suzuki and Y. Abe, J. Non-Cryst. Solids **43**, 141 (1981).

[50] R. Brückner, J. Non-Cryst. Solids **5**, 281 (1971).

[51] R. Simha and R. F. Boyer, J. Chem. Phys. **37**, 1003 (1962).

[52] M. Wyart, Ann. Phys.(N.Y.) **30**, 1 (2005).